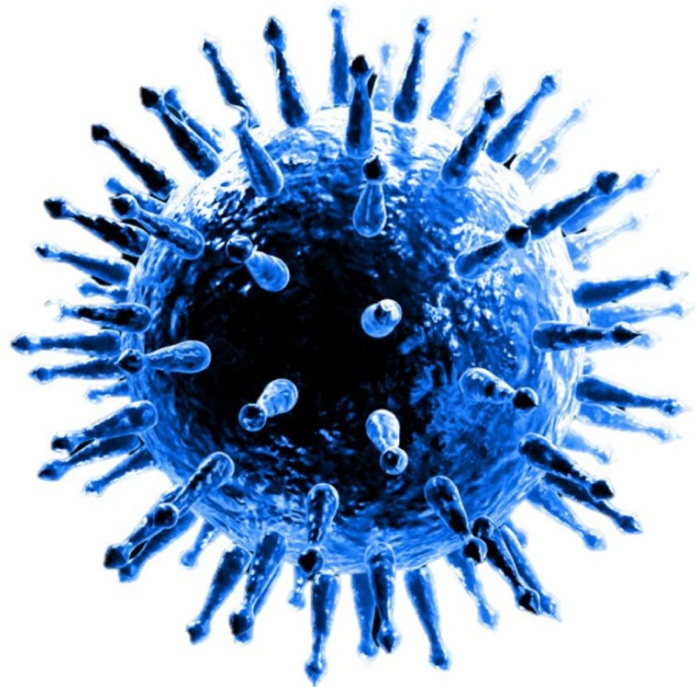


Comparing forecast performance on different synthetic pandemics

Grégoire Béchade

Internship at
Chalmers University
01/04/24 - 19/07/24



Under the supervision of
Philipp Gerlee

Contents

1	Plagiarism integrity statement	3
2	Introduction	4
3	Literature review and objectives	4
3.1	Literature review	4
3.2	Objectives	5
4	Generating synthetic pandemics	5
4.1	Covasim	5
4.2	First pandemics	6
4.3	Generating diverse pandemics	6
5	Models	11
5.1	The SIRH model	12
5.2	ARIMA and VAR models	13
5.3	The moving average model	14
5.4	Exponential regression	14
5.5	Machine learning models	15
5.6	Ensemble model	15
5.7	Computing confidence intervals on the prediction	16
6	Results and discussion	21
6.1	Point classification	22
6.2	Evaluation of the models	22
6.3	The Ensemble model	24
6.4	Summary of Key Findings	25
6.5	Test on real data	27
6.6	Comparison with Previous Research	27
6.7	Practical Implications	28
6.8	Limitations	28
7	Appendix	32

1 Plagiarism integrity statement

By this statement, I declare that the content of this work is fully original and has not been copied. Some previous results have been used, and they are always explicitly cited. Moreover, the work presented in this report led to a publication. Some parts of this report are directly taken from this publication, as they referred to the exact same work and results. Those parts were fully written by me, and present results based only on my personal work.

2 Introduction

The recent outbreak of COVID-19 has enlightened the importance of accurate forecasting models, for policymakers and population alike. The number of hospitalized individuals has shown to be a key indicator in the last pandemic, as maintaining the number of hospitalized individuals below the capacity of the healthcare system was a major concern. Predicting the trajectory of a pandemic is a complex task, considering the number of parameters that have an influence on the outbreak. I will relate in this report the work that was done during a research internship of 16 weeks at Chalmers University, whose goal was to develop predictive models and assess their performance on a set of diverse pandemics. The elaboration of the set of pandemics was also an important part of the work.

I implemented 13 individual models and an ensemble model to forecast the number of hospitalizations 7 and 14 days ahead, given the data up to the current day. These models are divided into two categories: those trained only on hospitalization data and those incorporating additional time-series such as mobility data and the number of infected agents. The individual models are: variations of the SIRH (Susceptible, Infected, Recovered, Hospitalized) model, ARIMA, VAR, moving average, exponential regressions, Bayesian and linear regressors.

A complex agent-based model was used to simulate pandemics of a wide diversity. By varying key parameters and using different mobility patterns, I created a diverse set of 324 synthetic pandemic scenarios (consisting of daily reports of key quantities). This diversity allows for a robust evaluation of the models across various conditions.

The models were trained and tested on many points of these pandemics, allowing for a consistent analysis of their performance. Additionally, I classified the points in the pandemic trajectories based on the reproductive number to understand model performance at different phases of the pandemic.

This project aims to determine the most consistent and reliable models for forecasting hospitalizations during pandemics, at different phases of the outbreak. Those predictions are not spatial or biological predictions, but forecasts of time series representing the evolution of key values in an area (number of hospitalized, of deaths...). By analyzing the performance of various models across a wide range of synthetic pandemic scenarios, the objective is to provide insights that can guide the selection and development of predictive models for real-world applications. The findings of this internship highlight the strengths and weaknesses of different modeling approaches and underscore the value of ensemble models in achieving robust and accurate predictions.

The simulations that are described in this report and lead to all the figures presented below are available on this [GitHub Repository](#).

3 Literature review and objectives

3.1 Literature review

The literature of pandemic forecasting is well documented, as many studies have been conducted during the outbreak of Covid 19. The huge amount of article published makes it difficult to

identify relevant articles with interesting results. The first part of the internship was dedicated to the analysis of the literature, to find useful ideas for the project, such as models, methods or clever ways to present the results. I found that early predictions on the number of cases (such as [4]) almost overestimated the real spread of the virus, and acknowledge the difficulty to estimate the impacts of governments strategies to mitigate the outbreak.

Some model performances were pointed out. Indeed, the autoregressive models such as the ARIMA model seem to outperform the other model in short-terms predictions ([10] and [18]), whereas compartmental models such as the SIR model are more performant for long-term predictions ([15]).

Many articles about the ensemble models were found ([2], [16], [7]). The ensemble models aggregate the predictions of many models, and output a function of these predictions. It can be simple functions (such as median), or more complexe ones such as stacking (as it is done in [16]) or linear opinion pool (see [7]). These studies all enhance the following results : the ensemble models are rarely the best, but never the last, when all the models are ranked together. Indeed, when compared to individual models, the ensemble models seem very consistent in their predictions, and their ranking distribution among the other models is very tight.

Many papers on the variations of SIR model were found ([5], [8], [19]) If this simple model does not manage to catch the complexity of an outbreak, some variations can have very good results. For instance, in [5], the authors manage to find a strong correlation between the mobility data and the number of cases, with a three weeks lag.

Other interesting results were also pointed out. For instance, [8] highlighted the relevance of testing to estimate the proportions of infected individuals. [19] focused on ICU occupancy for its predictive model, which is a key variable to monitor.

3.2 Objectives

After this review, a general direction was established. It was decided to implement some simple models (ARIMA, SIR, exponential regression...) to compare their performances across a wide range of pandemics. Indeed, the models that were found in the literature were often tested on a single pandemic, which might lead to a bias in the results and could limit their generalization.

4 Generating synthetic pandemics

To be able to compare the performances of the models, one needs pandemic data to compare them. As the objective was to obtain the most consistent results, I decided not to train and compare the models on real data as this data is limited and biased: the results would not have been relevant when facing a new pandemic. All the simulations in this paper are made on a fixed population of 10^6 agents.

4.1 Covasim

To generate the pandemics, Covasim [9], a python library that can simulate the evolution of a pandemic, was used. Covasim is an agent-based model that can simulate the spread of a

pandemic in a population. This model takes as an input many parameters such as the population type, the population size, the age distribution... and outputs a complete description of the pandemic, with real-time values of each relevant piece of information, such as the number of severe individuals, asymptomatic individuals... but also physical values such as the value of the reproduction number. Covasim enables to generate a wide diversity of pandemics, thanks to the plurality of parameters that can be given as inputs to the model, but also with interventions that can be planned by the user. These interventions can help assess the impact of a vaccination campaign, or lockdown scenarios. They represent relative changes in the probabilities of transmission. Covasim was used by policymakers during the Covid 19 outbreak to adapt their strategies of mitigation, for instance in Australia, Vietnam, India and United States ([9]).

4.2 First pandemics

For the implementation and the first tests of the models, two pandemics were generated. The first one focusing on the new deaths count and the second one focusing on the number of hospitalizations. I quickly decided to move to the second pandemic, as the variable 'new deaths' is neither relevant nor continuous (which caused problems in the implementation of some models, namely the SIRH models).

The different interventions were based on mobility reports from Västtrafik (see appendix 7), the public transport company of the city of Gothenburg. They were reported during the Covid 19 pandemic and have been retrieved in [5]. These interventions correspond to 53 relative weekly variations of the mobility, with a reference value of 1 for the first week of the report, which correspond to the 9-th week of 2020.

4.3 Generating diverse pandemics

In order to evaluate the performance of my models on a wide range of pandemics, I generated a training set of pandemics. A wide diversity of pandemics is needed to determine the most consistent model. It is so relevant to identify the key parameters that generate this diversity. As Covasim has a very huge set of inputs parameters, a first subset of key parameters was identified: the spread parameters and the severity parameters. The severity parameters are the 4 parameters that correspond to the probability for an agent to get from a compartment to another (for instance from infected to critical). The spread parameters are 9 parameters that represent the distribution of probability of the time spend by an agent in a compartment (such as infected, critical...) once he entered it. This set of 13 parameters is then noted as S . This distribution is a log-normal distribution, but the spread-parameters correspond to the mean of this log-normal distribution. All the parameters have a default value of 1, which corresponds to keeping the reference value. I decided to select 4 parameters and make them vary in $[0.5, 1, 2]$, leading to a set of 81 pandemics. To select the 4 parameters that generated the most diversity, various diversity metrics were computed.

Let $Y_1, Y_2 \in \mathbb{R}^n$ be two time series of n days representing the number of hospitalized individuals in two pandemics, Y' and Y'' the first and second derivatives of Y , and \tilde{Y} the normalized array of Y so that its maximum is equal to 1.

Let :

$$l_1(Y_1, Y_2) = \|Y_1 - Y_2\|_{L_1}$$

$$l_2(Y_1, Y_2) = \left\| \left(\frac{\max(Y_1)}{\max(Y_2)}, \frac{\max(Y_1')}{\max(Y_2')}, \frac{\max(Y_1'')}{\max(Y_2'')}, \|\tilde{Y}_1 - \tilde{Y}_2\|_{L_1}, \|\tilde{Y}_1' - \tilde{Y}_2'\|_{L_1}, \|\tilde{Y}_1'' - \tilde{Y}_2''\|_{L_1} \right) \right\|_{L_2}$$

$$l_3(Y_1, Y_2) = \mathcal{W}(\tilde{Y}_1 - \tilde{Y}_2), \text{ with } \mathcal{W} \text{ the Wasserstein distance ([13])}.$$

$$l_4(Y_1, Y_2) = \left\| \left(\frac{\max(Y_1)}{\max(Y_2)}, \frac{\max(Y_1')}{\max(Y_2')}, \frac{\max(Y_1'')}{\max(Y_2'')}, \mathcal{W}(\tilde{Y}_1 - \tilde{Y}_2), \mathcal{W}(\tilde{Y}_1' - \tilde{Y}_2'), \mathcal{W}(\tilde{Y}_1'' - \tilde{Y}_2'') \right) \right\|_{L_2}$$

To determine which measure to use, I generated 14 pandemics. Each pandemic but the last one has default parameters except one of them which was doubled. The last pandemic has only default parameters.

For each norm l_k , I determined s , the subset of 4 pandemics that maximized the following quantity:

$$\mathcal{L}_k(s) = \sum_{i,j \in s, i \neq j} l_k(Y_i, Y_j)$$

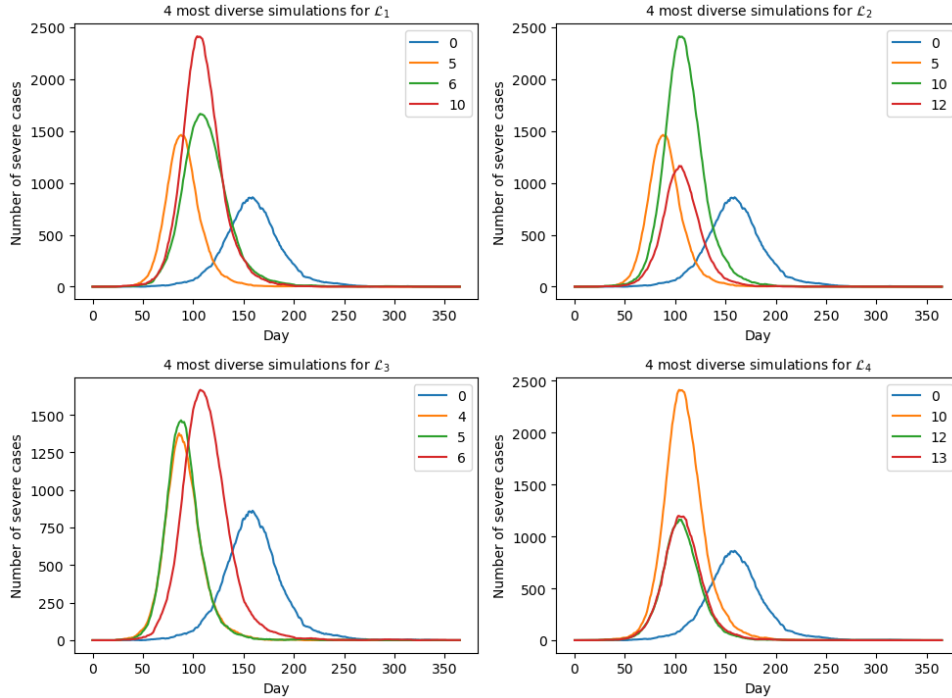


Figure 1: 4 most diverse pandemics according to each norm.

The 4 most diverse pandemics (in the subset of 14 pandemics generated) according to each norm are shown in the Fig.1. As "diversity" is not countable, a human choice was necessary to choose the most relevant norm. According to Fig. 1, I decided to select l_2 . But, keeping the parameters $[0, 5, 10, 12]$ would not be accurate, as the parameters were changed independently, and the diversity did not take into account the correlation between some of them.

Finding the parameters that maximise the \mathcal{L} diversity is equivalent to solve the following problem :

$s_{opt} = \operatorname{argmax}_{s \in S, |s|=4} \mathcal{L}(s)$, with $\mathcal{L}(s) = \sum_{p_1, p_2 \in \mathcal{P}_g(s)} l_2(p_1, p_2)$, and $\mathcal{P}_g(s)$ the set of the 81 pandemics generated with the 4 parameters of s .

However, generating a pandemic with **Covasim** is time consuming, and it is not possible to compute the diversity of each set of 4 parameters s included in S (the set of all 13 parameters).

A MCMC algorithm [3] was then implemented, to perform a clever grid search on the different subsets $s \subset S$ of parameters. The MCMC algorithm is a method which is used to sample from a distribution that can't be directly sampled. The main idea is to construct a Markov Chain whose stationary distribution is the objective distribution.

Let $\mathcal{S} = \{s \subset S; |s| = 4\}$ be the support of the target distribution, which is, in our case, the set of all the 715 combinations of the 4 parameters among the 13 different possible, and let π be the target distribution on \mathcal{S} . $\forall s \in \mathcal{S}, \pi(s) = \frac{\mathcal{L}(s)}{\sum_{s \in \mathcal{S}} \mathcal{L}(s)}$. π is not directly computable as it is too time consuming to compute the denominator. We suppose that $\forall s \in \mathcal{S}, \mathcal{L}(s) > 0$. It is a reasonable assumption, as $\mathcal{L}(s) = 0$ means that the 81 pandemics generated are strictly identical.

For each $s = [a, b, c, d] \in \mathcal{S}$, let $ne(s)$ be the set of the neighbours of s , i.e the set of all the elements of \mathcal{S} who have only one parameter different from s . For instance, $[0, 3, 9, 12] \in ne([0, 3, 10, 12])$, but $[0, 3, 9, 12] \notin ne([0, 3, 8, 10])$.

Let U_n be a sequence of independent uniform random variables on $[0, 1]$ and $\forall s \in \mathcal{S}$, let $U_n^{ne(s)}$ be a sequence of independent uniform random variables on $ne(s)$. Let $s_0 \in \mathcal{S}$ and let S_n be the random sequence defined as follow :

$$\begin{cases} S_0 = s_0 \\ \forall n \in \mathbb{N}, \alpha_n = \frac{\mathcal{L}(U_n^{ne(S_n)})}{\mathcal{L}(S_n)} \\ \forall n \in \mathbb{N}, S_{n+1} = U_n^{ne(S_n)} \mathbb{1}_{\{U_n < \alpha_n\}} + S_n \mathbb{1}_{\{U_n > \alpha_n\}} \end{cases}$$

This formula means that at each iteration, a neighbor of S_n is uniformly selected among all the neighbours of S_n (it is $U_n^{ne(S_n)}$). The Markov Chain moves to this neighbor if the value of $\mathcal{L}(U_n^{ne(S_n)})$ is higher than the value of the function $\mathcal{L}(S_n)$ at the current state. If the new value of \mathcal{L} is smaller, the Markov Chain moves with a probability that is equal to the ratio of the two values. This way of moving on the different subsets prevents to be stuck in a local maxima but avoids exploring dummies areas, in which the diversity is very small.

As S_{n+1} is a function of S_n and of other independent random variables, the sequence S_n is a homogeneous Markov Chain.

The transition matrix of this Markov Chain is the following:

$$K(s, s') : \begin{cases} 0 & \text{if } s' \notin ne(s) \text{ and } s' \neq s \\ \frac{1}{Card(ne(s))} = \frac{1}{36} & \text{if } s' \in ne(s) \text{ and } \frac{\mathcal{L}(s')}{\mathcal{L}(s)} > 1 \text{ and } s' \neq s \\ \frac{1}{36} \times \frac{\mathcal{L}(s')}{\mathcal{L}(s)} & \text{if } s' \in ne(s) \text{ and } \frac{\mathcal{L}(s')}{\mathcal{L}(s)} \leq 1 \text{ and } s' \neq s \\ 1 - \sum_{s' \in \mathcal{S}, s' \neq s} K(s, s') & \text{if } s' = s \end{cases}$$

Let $(s, s') \in \mathcal{S}^2$. Suppose that $s' \neq s$, that $s' \in ne(s)$, and that $\mathcal{L}(s) < \mathcal{L}(s')$ (the other case is symmetric).

$$\begin{aligned} \pi(s)K(s, s') &= \frac{\mathcal{L}(s)}{\sum_{s \in \mathcal{S}} \mathcal{L}(s)} \times \frac{1}{36} \quad \text{as } \mathcal{L}(s) < \mathcal{L}(s') \\ &= \frac{\mathcal{L}(s)}{\sum_{s \in \mathcal{S}} \mathcal{L}(s)} \times \frac{1}{36} \times \frac{\mathcal{L}(s')}{\mathcal{L}(s')} \\ &= \frac{\mathcal{L}(s')}{\sum_{s \in \mathcal{S}} \mathcal{L}(s)} \times \frac{1}{36} \times \frac{\mathcal{L}(s)}{\mathcal{L}(s')} \\ &= \pi(s')K(s', s) \end{aligned}$$

Indeed, each subset s has 36 neighbourh, as there are 13 parameters and one can replace each parameter of s by any of the 9 others.

If $s' \notin ne(s)$, then $s \notin ne(s')$ and $K(s, s') = 0$. We directly have $\pi(s)K(s, s') = 0 = \pi(s')K(s', s)$.

Thus, π is **reversible** for K .

Let $(s, s') \in \mathcal{S}^2$. Let us note (a, b, c, d) and (a', b', c', d') the elements of s and s' . We note :

$$\begin{aligned} s_1 &= [a', b, c, d] \\ s_2 &= [a', b', c, d] \\ s_3 &= [a', b', c', d] \end{aligned}$$

$$\begin{aligned}
\mathbb{P}(S_{n+4} = s' | S_n = s) &\geq \mathbb{P}(S_{n+4} = s' \cap S_{n+3} = s_3 \cap S_{n+2} = s_2 \cap S_{n+1} = s_1 | S_n = s) \\
&\geq \mathbb{P}(S_{n+4} = s' | S_{n+3} = s_3 \cap S_{n+2} = s_2 \cap S_{n+1} = s_1 \cap S_n = s) \\
&\quad \times \mathbb{P}(S_{n+3} = s_3 \cap S_{n+2} = s_2 \cap S_{n+1} = s_1 | S_n = s) \text{ (Baye's Formula)} \\
&\geq \mathbb{P}(S_{n+4} = s' | S_{n+3} = s_3) \\
&\quad \times \mathbb{P}(S_{n+3} = s_3 \cap S_{n+2} = s_2 \cap S_{n+1} = s_1 | S_n = s) \text{ (by Markov's property)} \\
&\vdots \\
&\geq \mathbb{P}(S_{n+4} = s' | S_{n+3} = s_3) \times \mathbb{P}(S_{n+3} = s_3 | S_{n+2} = s_2) \times \mathbb{P}(S_{n+2} = s_2 | S_{n+1} = s_1) \\
&\quad \times \mathbb{P}(S_{n+1} = s_1 | S_n = s) \text{ (by Markov's property)} \\
&\geq \left(\frac{1}{36}\right)^4 \times \min(1, \frac{\mathcal{L}(s')}{\mathcal{L}(s)}) \times \min(1, \frac{\mathcal{L}(s_3)}{\mathcal{L}(s_2)}) \times \min(1, \frac{\mathcal{L}(s_2)}{\mathcal{L}(s_1)}) \times \min(1, \frac{\mathcal{L}(s_1)}{\mathcal{L}(s)}) \\
&> 0
\end{aligned}$$

Thus, S_n is **irreducible**.

A Markov chain of transition matrix P on the support \mathcal{S} is said to be *aperiodic* if:
 $\forall s \in \mathcal{S}, \forall s' \in \mathcal{S}, \exists N \in \mathbb{N}, \text{ s.t } \forall n > N, P(s, s')^n > 0$ [1]

First, note that $\forall s \in \mathcal{S}$, s is a local minimum (i.e if $\forall s' \in ne(s), \mathcal{L}(s') > \mathcal{L}(s)$) if and only if $K(s, s) = 0$

Thus, if s is not a local minimum, then $K(s, s) > 0$. Moreover, $\forall s \in \mathcal{S}, \forall s' \in ne(s)$, if $s \neq s'$, then $K(s, s') \neq 0$

Let $(s, s') \in \mathcal{S}^2$.

- If s' is not a local minimum,
 $\forall n > 4, \mathbb{P}(S_n = s' | S_0 = s) \geq \mathbb{P}(S_4 = s' | S_0 = s) \times K(s', s')^{n-4} > 0$
- If s' is a local minimum, $\forall s^* \in ne(s')$, s^* is not a local minimum and $K(s^*, s^*) \neq 0$.
 $\forall n > 5, \mathbb{P}(S_n = s' | S_0 = s) \geq \mathbb{P}(S_3 = s^* | S_0 = s) \times K(s^*, s^*)^{n-4} \times K(s^*, s') > 0$

Thus S_n is an **aperiodic** Markov Chain.

Finally, according to the **Theorem 5.5** from [1], as S_n is irreducible and aperiodic, as π is the stationary distribution, and as \mathcal{S} is countable, S_n converges in distribution toward π .

The most probable set that will be sampled by S_n is the one that maximises the diversity. I implemented this MCMC algorithm to maximise \mathcal{L} on \mathcal{S} . The first value of the sequence was a clever starting point: the four parameters that maximized \mathcal{L} on the 14 pandemics generated earlier (Fig.1). After 200 iterations, the set of parameters that maximised the diversity was [2, 4, 9, 10], which correspond to the parameters [sym2sev, asym2rec, rel_symp_prob,

`rel_severe_prob`]. They correspond respectively to the mean of the log-normal distribution representing the time spent in the compartment 'symptomatic' before moving into the compartment 'severe', the mean of the log-normal distribution representing the time spent in the compartment 'asymptomatic' before moving into the compartment 'recovered', to the scale factor for proportion of symptomatic cases and to the scale factor for proportion of symptomatic cases that become severe. (see [9]). The \mathcal{L} -diversity increased from 62353 to 93553.

To create the most diverse set possible, I used 4 different mobilities reports (Fig.2), corresponding to constant mobility, annual variations, lockdown scenario and the reports from Västtraffik from [5] (see 4.2). These time-varying mobilities enabled us to model more complex

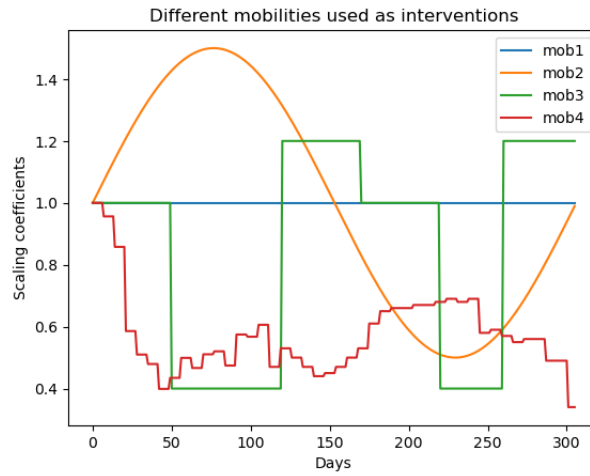


Figure 2: Mobility reports.

behaviours of the pandemics. I finally modelled 324 pandemics. Indeed each of the 4 parameters was scaled among 3 values : [0.5, 1, 2] and the 4 mobilities reports were used.

5 Models

In this study, let us define a model h_θ as a function h defined on \mathbb{N} , with parameter θ and trained on the data \mathcal{D} . In the training phase, $\hat{\theta}$, an estimator of θ is computed from \mathcal{D} , and used for the prediction. I designed two types of models: the first type corresponds to models which are only trained on the time series we want to predict (the number of hospitalized individuals in our case), and models of the second type are trained on the same time series, but also on other time series that can be relevant to forecast the number of hospitalized (the mobility and the number of infected). All of these models were implemented in Python, and are available on the Github repository provided with this report (2). During the training or prediction phase, the computation sometimes fails (for instance, when the matrix is non-invertible for the linear regression model). The model then outputs the predicted value of the moving average model (see Sec.5.3), which can be interpreted as a naive output when the computation fails.

Task of a model:

Each model h is given:

1. A training set \mathcal{D} of size n .
2. A reach of prediction r
3. A confidence threshold α

And outputs:

1. A prediction \hat{Y}_{n+r}
2. A $(1 - \alpha)$ confidence interval on the prediction, $I_{\alpha, n+r}$

The model will train on the data \mathcal{D} to compute $\hat{\theta}$, the parameter estimator and the output $\hat{Y}_{n+r} = h_{\hat{\theta}}(n + r)$.

5.1 The SIRH model

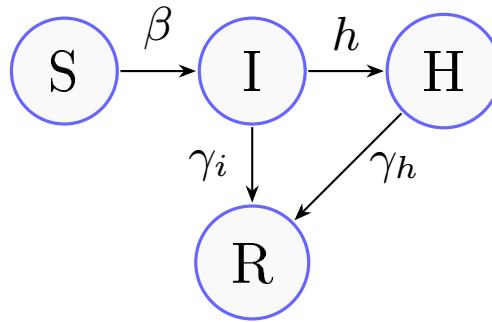


Figure 3: Scheme of the SIRH model

The SIRH model (Fig.3) is an extension of the classic compartmental SIR (Susceptible-Infectious-Recovered) model used to describe the spread of infectious diseases. In the SIRH model, a fourth compartment, "H" for "Hospitalized," is added. Each compartment corresponds to the number of people in the state of health of the compartment. The evolution of the number of people in each compartment is described by a system of ordinary differential equations:

$$\begin{cases} \frac{dS}{dt} = -\beta \frac{SI}{N} \\ \frac{dI}{dt} = \beta \frac{SI}{N} - \gamma_i I - hI \\ \frac{dR}{dt} = \gamma_i I + \gamma_h h \\ \frac{dH}{dt} = hI - \gamma_h H \end{cases} \quad (1)$$

At $t = 0$, the values of (S_0, I_0, R_0, H_0) are fixed to $(10^6 - 1, 1, 0, 0)$. As the system of equation can't be directly solved, we use a Euler's method to solve it.

To train this model, we minimize the least squares error between the curve of the number of hospitalized predicted by the model $\text{SIRH}(\theta)$ to the curve of the number of hospitalized of the

training data with respect to $\theta = (\beta, \gamma_i, \gamma_h, h)$. I implemented some variations of the model in which γ_i , γ_h or both were fixed to the value 0.2 (see the Table.1). This value of 0.2 seems arbitrary but corresponds to an expected value of recovery of 5 days and sometimes helps the curve fit function to converge, as the computations sometimes fail to optimize on the 4 parameters.

	γ_i	γ_h
SIRH1	0.2	0.2
SIRH2	0.2	free
SIRH3	free	0.2
SIRH4	free	free

Table 1: Difference between the SIRH models

In the prediction phase, an r day SIRH simulation is launched, with the parameter $\hat{\theta}$ computed during the training phase. The initial values for S and I correspond to the last value of the fit from the training phase. The initial value for H corresponds to the last value of \mathcal{D} , the training data. The initial value of R is fixed by the previous values, as the equation $S_t + I_t + R_t + H_t = N$ is always true. The confidence interval of the prediction is computed using a linearization and the use of the delta-method (see Sec.5.7)

An SIRH model of the second type was implemented. It has the same structure but uses the mobility data and the number of infected to be more precise. The idea is the same, but there are two differences:

- β varies with the time as a linear combination of the mobility: $\beta_t = a + b \times m_t$ (which is inspired from [5])
- The data is fitted to both the number of hospitalized and the number of infected.

To write it more formally, let $H_\theta(t)$ and $I_\theta(t)$ be the number of hospitalized and infected at time t in the SIRH model with parameters θ . Let $Y_{H,t}$ and $Y_{I,t}$ be the number of hospitalized and infected at time t in the data. We have:

$$\hat{\theta} = \underset{\theta \in \mathbb{R}^5}{\operatorname{argmin}} \sum_{t=1}^n \left(\frac{H_\theta(t) - Y_{H,t}}{\max(Y_{H,t})} \right)^2 + \left(\frac{I_\theta(t) - Y_{I,t}}{\max(Y_{I,t})} \right)^2$$

With $\theta = (a, b, \gamma_i, \gamma_h, h)$ and m_t the mobility at time t . The normalization factors prevent the optimization to focus on the number of infected, which is bigger than the number of hospitalized. During my first tries, I hadn't normalized the data and the curve of the infected was almost perfectly fitted to the curve of the SIRH model, but the curve of the hospitalized was flat. Once again, a variation of the SIRH model was implemented, in which the value of γ_h and γ_i is fixed to 0.2. SIRH multi 1 refers to the model in which γ_h and γ_i are free and SIRH multi 2 refers to the model in which γ_h and γ_i are fixed to 0.2.

5.2 ARIMA and VAR models

The ARIMA and VAR models are used for time-series forecasting and have outperformed many models in pandemic forecasting (see [10] and [18]). The $ARIMA(p, d, q)$ model is the sum of an $AR(p)$ and a $MA(q)$ model applied on the time series differentiated d times. It follows the

equation:

$$Y_t^d = \alpha + \sum_{i=1}^p \beta_{t-i} Y_{t-i}^d + \sum_{j=1}^q \phi_{t-j} \epsilon_{t-j}$$

where Y_t^d is the time series at time t , d is the order of the differentiation, α is a constant, p is the order of the autoregressive part, q is the order of the moving average part and ϵ_{t-j} is the difference between the prediction of the model and the real value at time $t - j$.

The coefficients are estimated through maximum likelihood estimation. This method is implemented in the `statsmodels` library, which directly provides prediction and confidence intervals. I performed a grid search on a single pandemic to identify the combination of parameters that would optimize the prediction accuracy. I found an optimal value for $p = 3, d = 0, q = 3$.

The VAR model is a multi-dimensional *AR* model, in which different variables are predicted. It therefore corresponds to a second type model. This model exploits the correlation between variables and the values of the parameters of a VAR have physical sense as they can be interpreted to find correlations between variables. Let $Y_{1,t}, \dots, Y_{k,t}$ be the times series (in our case, $k = 3$ and they correspond to the number of hospitalized, the number of infected and the mobility data).

$$\begin{aligned} \text{VAR}(p) : \begin{pmatrix} Y_{1,t} \\ Y_{2,t} \\ \vdots \\ Y_{k,t} \end{pmatrix} &= \begin{pmatrix} c_1 \\ c_2 \\ \vdots \\ c_k \end{pmatrix} + \begin{pmatrix} \phi_{11,1} & \phi_{12,1} & \cdots & \phi_{1k,1} \\ \phi_{21,1} & \phi_{22,1} & \cdots & \phi_{2k,1} \\ \vdots & \vdots & \ddots & \vdots \\ \phi_{k1,1} & \phi_{k2,1} & \cdots & \phi_{kk,1} \end{pmatrix} \begin{pmatrix} Y_{1,t-1} \\ Y_{2,t-1} \\ \vdots \\ Y_{k,t-1} \end{pmatrix} \\ &+ \cdots + \begin{pmatrix} \phi_{11,p} & \phi_{12,p} & \cdots & \phi_{1k,p} \\ \phi_{21,p} & \phi_{22,p} & \cdots & \phi_{2k,p} \\ \vdots & \vdots & \ddots & \vdots \\ \phi_{k1,p} & \phi_{k2,p} & \cdots & \phi_{kk,p} \end{pmatrix} \begin{pmatrix} Y_{1,t-p} \\ Y_{2,t-p} \\ \vdots \\ Y_{k,t-p} \end{pmatrix} + \begin{pmatrix} \epsilon_{1,t} \\ \epsilon_{2,t} \\ \vdots \\ \epsilon_{k,t} \end{pmatrix} \end{aligned}$$

Again, the $\phi_{i,j,k}$ and c_i are estimated through maximum likelihood estimation with the `statsmodels` library. The confidence intervals are also directly provided by the library.

5.3 The moving average model

A mere moving average model was also implemented. It returns a constant prediction that corresponds to the mean of the past 7 days. The confidence intervals are computed by assuming that the predictions follow a normal distribution of variance equal to the variance of the last 7 data points. This model is used as a baseline. Indeed, a model that does not manage to outperform the moving average model would not be useful.

5.4 Exponential regression

An exponential regression model was implemented. It corresponds to fitting the data of the number of hospitalized (Y_t) to the function $E_{a,b,c}(t) = a \times e^{bt} + c$. The value of $\theta = (a, b, c)$ is computed through a least squares minimization method. The confidence interval for the prediction is estimated using the same method as SIRH (see Sec.5.7).

An exponential regression of the second type was also implemented:

The data of the number of hospitalized is fitted to the function $E_{a,b,c,d,e}(t) = a \times e^{bm_{t-i} + ct + d \times \ln f_{t-j}} + e$.

m_t is the mobility data at time t and inf_t is the number of infected at time t . The value of $\theta = (a, b, c, d, e)$ is computed through a least squares method. The optimal value of the time lag i and j is optimized during the training phase through a grid search among all the values between 0 and 14. The confidence interval for the prediction is estimated using the same method as SIRH (see Sec.5.7).

5.5 Machine learning models

In order to implement machine learning regressors, I converted the time-series $Y_{t,t \in \{1, \dots, n\}}$ in a training set (X_i, Y_i) such that:

$$\forall i \in \{21, \dots, n\}, X_i = (Y_{i-1}, Y_{i-2}, \dots, Y_{i-20}).$$

I have then trained and optimized both regressors: the linear and the bayesian regressors, which were the only ones that did not output absurd results among the **scikit-learn** models among: linear regression, bayesian regression, Gradient boosting regressor, Random Forest regressor and SVR. The Bayesian Ridge model was implemented with the default prior of the **scikit-learn** library (a gamma distribution with shape parameter 10^{-6} and scale parameter 10^{-6}). The confidence interval for the linear regression prediction was computed as follows:

Let us suppose that the data follows a linear regression model: $Y = X\beta + \epsilon$, with $Y \in \mathbb{R}^n$, $X \in \mathbb{R}^{n \times d}$, $\beta \in \mathbb{R}^d$ and $\epsilon \in \mathbb{R}^n$ and $\forall i \in \{1, \dots, n\}, \epsilon_i \sim \mathcal{N}(0, \sigma^2)$ iid. The least squares estimator of β is $\hat{\beta} = (X^T X)^{-1} X^T Y$. If we have new data $\tilde{X} \in \mathbb{R}^{1 \times d}$ that we want to predict, the prediction is:

$$\begin{aligned} \tilde{Y} &= \tilde{X} \hat{\beta} \\ &= \tilde{X} (X^T X)^{-1} X^T Y \\ &= \tilde{X} (X^T X)^{-1} X^T (X\beta + \epsilon) \\ &= \tilde{X} \beta + \tilde{X} (X^T X)^{-1} X^T \epsilon. \end{aligned}$$

\tilde{Y} follows a normal distribution of expected value $\tilde{X} \beta$ and variance $\tilde{X} (X^T X)^{-1} \tilde{X}^T \sigma^2$.

The confidence interval for bayesian regression was directly computed with the variance of the parameters given by the scikit-learn library and the delta method.

5.6 Ensemble model

It has been shown (see [2] and [16]), that ensemble models, which combine the outputs of many models, can outperform by far individual models. I have implemented an ensemble model which is a linear combination of the outputs of the 13 models described above, with the exponential models removed. The weights of this model were found by minimizing the least-squared error between the prediction of the ensemble model and the real value of the number of hospitalized on a train set of approximately 80% of the generated pandemic. They are represented in Fig.4. As the ensemble model only outputs a single value without confidence intervals, it is only evaluated with the RMSE metric.

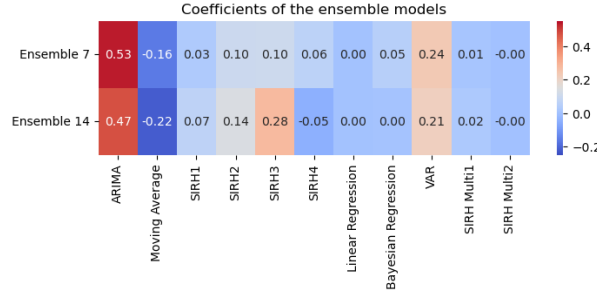


Figure 4: Weights of the ensemble models

5.7 Computing confidence intervals on the prediction

In this section, we prove the formula used in the code to compute the confidence intervals. The following proof is inspired from [17] and [14]. I have assembled individual proofs from these two articles to get the final results. Some notations and steps are identical to what one can find in the papers and are explicitly cited.

This problem is a non linear regression problem. The proof is made of three steps. First, we linearize the problem around the solution to get back to a linear regression problem. Then, we show that the estimator of the linear regression problem is asymptotically normal. Finally, we use the delta-method to obtain the asymptotic normality of the non linear regression estimator .

Assumption:

We suppose that the data of the pandemic observed follows the model h , of parameter $\theta^* \in \mathbb{R}^d$. Let $Y_{i,i=1,\dots,n}$ be the number of hospitalized at each day. We suppose that: $Y_i = h_{\theta^*}(i) + \epsilon_i$, with $\epsilon_i \sim \mathcal{N}(0, \sigma^2)$, iid, and independent from all the other variables. The objective is to estimate θ^* . We use $\hat{\theta}$, the least squares estimator of θ^* as an estimator of θ^* :

$$\hat{\theta} = \underset{\theta \in \mathbb{R}^d}{\operatorname{argmin}} \sum_{i=1}^n (Y_i - h_{\theta}(i))^2$$

This problem is a non-linear regression problem on the regressors i . We also suppose that h_{θ} is differentiable. Finally, we assume that

$$\exists A_0 \in \mathbb{R}^{1 \times d}, \frac{1}{n} \sum_{i=1}^n \nabla_{\theta} h_{\theta^*}(i) \nabla_{\theta} h_{\theta^*}(i)^T \xrightarrow{n \rightarrow +\infty} A_0^T A_0. \quad (2)$$

STEP 1:

Let:

$$Y = \begin{pmatrix} Y_1 \\ \vdots \\ Y_n \end{pmatrix}$$

$$h_\theta = \begin{pmatrix} h_\theta(1) \\ \vdots \\ h_\theta(n) \end{pmatrix}$$

We have:

$$\hat{\theta} = \underset{\theta \in \mathbb{R}^d}{\operatorname{argmin}} \|Y - h_\theta\|^2$$

Now, if θ is close enough to θ^* , we can write (from [17]):

$$\forall i \in \{1, \dots, n\} : h_\theta(i) = h_{\theta^*}(i) + (\theta - \theta^*)^T \nabla_\theta h_{\theta^*}(i)$$

which leads to:

$$\hat{\theta} = \underset{\theta \in \mathbb{R}^d}{\operatorname{argmin}} \|Y - h_{\theta^*} - (\theta - \theta^*)^T \nabla_\theta h_{\theta^*}\|^2$$

Let us define (from [17]):

$$\tilde{Y} = Y - h_{\theta^*}$$

$$\beta = \theta - \theta^*$$

$$\hat{\beta} = \theta - \hat{\theta}$$

and let us define the matrix $A \in \mathbb{R}^{n \times d}$ such that $\forall i \in \{1, \dots, n\}, \forall j \in \{1, \dots, d\}, A_{i,j} = \frac{dh_{\theta^*}}{d\theta_j}(i)$. ([17])

The previous problem can be re-written as:

$$\hat{\beta} = \underset{\beta \in \mathbb{R}^d}{\operatorname{argmin}} \|\tilde{Y} - A\beta\|^2$$

This is now a linear regression problem on the regressors $\nabla_\theta h_{\theta^*}(i)$.

STEP 2:

Let us solve this problem in the general case.

Let (A_i, \tilde{Y}_i) be the observations. In our case, $A_i = (\nabla_\theta h_{\theta^*}(i))^T$, the rows of A , and is a fixed quantity. Let us assume that $\tilde{Y}_i = A_i \beta^* + \epsilon'_i$, with $\epsilon'_i \sim \mathcal{N}(0, \sigma'^2)$.

The solution of this problem is explicitly (from [14]):

$$\hat{\beta} = (A^T A)^{-1} A^T \tilde{Y}$$

This least-squares estimator is unbiased:

$$\mathbb{E}[\hat{\beta}] = \beta^*$$

$$\begin{aligned}\hat{\beta} &= \left(\sum_{i=1}^n A_i^T A_i \right)^{-1} \times \left(\sum_{i=1}^n A_i^T \tilde{Y}_i \right) \\ \hat{\beta} &= \frac{n}{n} \left(\sum_{i=1}^n A_i^T A_i \right)^{-1} \times \left(\sum_{i=1}^n A_i^T \tilde{Y}_i \right) \\ \hat{\beta} &= \left(\frac{1}{n} \sum_{i=1}^n A_i^T A_i \right)^{-1} \times \left(\frac{1}{n} \sum_{i=1}^n A_i^T \tilde{Y}_i \right)\end{aligned}$$

Let us denote, with the notations from [14]:

$$\hat{D} = \frac{1}{n} \sum_{i=1}^n A_i^T A_i, \quad \text{and} \quad \hat{\delta} = \left(\frac{1}{n} \sum_{i=1}^n A_i^T \tilde{Y}_i \right)$$

We have:

$$\hat{\beta} = \hat{D}^{-1} \hat{\delta}$$

$$\hat{D} \xrightarrow[a.s.]{} D, \text{ with } D = \mathbb{E}[A_i^T A_i] = A_0^T A_0 \text{ (cf Hyp 2)}$$

$\hat{\delta}$ is the empirical mean of random variables independent but non identically distributed. We therefore cannot use the Kolmogorov's strong law of large numbers. There exists a law of large number for independent and non identically distributed random variables, which asserts that (see Theorem 12 from [20]):

Theorem 1. *Let (X_k) be a sequence of independent random variables such that:*

1. *For all $k \geq 1$, $\mathbb{E}(X_k^2) < +\infty$;*
2. *There exists an increasing sequence (a_k) of strictly positive real numbers tending to infinity, such that*

$$\sum_{k=1}^{+\infty} \frac{\text{Var}(X_k)}{a_k^2} < +\infty.$$

Then, $\frac{S_n - \mathbb{E}S_n}{a_n}$ converges almost surely to 0. If additionally $a_n^{-1} \mathbb{E}S_n \rightarrow m$, then $\frac{S_n}{a_n}$ converges almost surely to m .

Let $i \in \{1, \dots, n\}$.

$$X_i = A_i^T \tilde{Y}_i = A_i^T A_i \beta^* + A_i^T \epsilon'_i.$$

The random values X_i are independent random variables.

$$\forall i \in \{1, \dots, n\}, \mathbb{E}[X_i^2] = \mathbb{E}[X_i]^2 + A_0^T A_0 \sigma'^2 < +\infty.$$

$$\sum_{i=1}^{\infty} \frac{\text{Var}(X_i)}{i^2} = \sum_{i=1}^{\infty} \frac{A_0^T A_0 \sigma'^2}{i^2} = A_0^T A_0 \sigma'^2 \sum_{i=1}^{\infty} \frac{1}{i^2} < +\infty.$$

$$\text{Moreover, } \frac{1}{n} \sum_{i=1}^n \mathbb{E}[X_i] = \frac{1}{n} \sum_{i=1}^n A_i^T A_i \beta^* = \frac{\beta^*}{n} \sum_{i=1}^n A_i^T A_i \xrightarrow[n \rightarrow \infty]{} \beta^* A_0^T A_0 \text{ (see 2).}$$

Therefore, with Theorem 1, we have: $\frac{1}{n} \sum_{i=1}^n A_i^T \tilde{Y}_i \xrightarrow[a.s.]{} \beta^* A_0^T A_0$

$$\hat{\delta} \xrightarrow[a.s.]{} \delta = A_0^T A_0 \beta^*$$

$\hat{\beta} = \hat{D}^{-1} \hat{\delta} \xrightarrow[a.s.]{} D^{-1} \delta$, as the following function ϕ is continuous:

$$\phi : \begin{cases} \mathcal{GL}_n(\mathbb{R}) & \rightarrow \mathcal{GL}_n(\mathbb{R}) \\ M & \mapsto M^{-1} \end{cases}$$

Now, let us show that $\hat{\beta}$ is asymptotically normal (proof from [14]):

$$\begin{aligned} \sqrt{n}(\hat{\beta} - \beta^*) &= \sqrt{n}(\hat{D}^{-1} \hat{\delta} - \beta^*) \\ &= \sqrt{n}(\hat{D}^{-1} \hat{\delta} - \hat{D}^{-1} \hat{D} \beta^*) \\ &= \sqrt{n} \hat{D}^{-1} (\hat{\delta} - \hat{D} \beta^*) \\ &= \sqrt{n} \hat{D}^{-1} \left(\frac{1}{n} \sum_{i=1}^n A_i^T \tilde{Y}_i - \frac{1}{n} \sum_{i=1}^n A_i^T A_i \beta^* \right) \\ &= \frac{\sqrt{n}}{n} \hat{D}^{-1} \left(\sum_{i=1}^n A_i^T (\tilde{Y}_i - A_i \beta^*) \right) \\ &= \frac{1}{\sqrt{n}} \hat{D}^{-1} \left(\sum_{i=1}^n A_i^T \epsilon_i \right) \end{aligned}$$

This line is made of two terms. Let's show that each one of them converges in law.

$$\begin{aligned} \frac{1}{\sqrt{n}} \left(\sum_{i=1}^n A_i^T \epsilon'_i \right) &= \sqrt{n} \left(\frac{1}{n} \sum_{i=1}^n A_i^T \epsilon'_i \right) \\ &= \sqrt{n} \left(\frac{1}{n} \sum_{i=1}^n A_i^T \epsilon'_i - 0 \right) \\ &\xrightarrow{\mathcal{L}} \mathcal{N}(0, \text{Var}(A_i^T \epsilon_i)) \end{aligned}$$

Yet, as ϵ_i and A_i are independent, and $\mathbb{E}[A_i^T \epsilon'_i] = 0$, $\text{Var}(A_i^T \epsilon_i) = \mathbb{E}[A_i^T A_i \epsilon_i^2] = \mathbb{E}[A_i^T A_i] \sigma'^2 = A_0^T A_0 \sigma'^2$.

Finally, $\frac{1}{\sqrt{n}} \left(\sum_{i=1}^n A_i^T \epsilon'_i \right) \xrightarrow{\mathcal{L}} \mathcal{N}(0, D \sigma'^2)$.

On the other hand, $\hat{D}^{-1} \xrightarrow{\mathcal{L}} D^{-1}$, which is constant.

Finally, by Slutsky's theorem, we obtain that :

$$\begin{aligned}\sqrt{n}(\hat{\beta} - \beta^*) &\xrightarrow{\mathcal{L}} D^{-1}\mathcal{N}(0, D\sigma'^2) \\ &\xrightarrow{\mathcal{L}} \mathcal{N}(0, D^{-1}(D\sigma'^2)(D^{-1})^T) \\ &\xrightarrow{\mathcal{L}} \mathcal{N}(0, D^{-1}D\sigma'^2(D^{-1})^T) \\ &\xrightarrow{\mathcal{L}} \mathcal{N}(0, \sigma'^2 D^{-1}) \\ &\xrightarrow{\mathcal{L}} \mathcal{N}(0, \sigma'^2 (A_0^T A_0)^{-1})\end{aligned}$$

Let's get back to the first problem:

As $\beta^* = 0$ and $\hat{\beta} = \hat{\theta} - \theta^*$, we have:

$$\sqrt{n}(\hat{\theta} - \theta^*) \xrightarrow{\mathcal{L}} \mathcal{N}(0, \sigma^2 (A_0^T A_0)^{-1})$$

and,

$$\hat{\theta} \sim \mathcal{N}(\theta^*, \frac{\sigma^2}{n} (A_0^T A_0)^{-1})$$

As a partial conclusion, we have that $\hat{\theta}$ is asymptotically normal.

STEP 3:

Let Σ be the covariance matrix estimated from the computation of $\hat{\theta}$.

As $\hat{\theta}$ is asymptotically normal, we can apply the delta-method:

$$\begin{aligned}\sqrt{n}(\hat{\theta} - \theta^*) &\xrightarrow{\mathcal{L}} \mathcal{N}(0, \Sigma) \\ \sqrt{n}(h_{\hat{\theta}} - h_{\theta^*}) &\xrightarrow{\mathcal{L}} \mathcal{N}(0, \nabla_{\theta} h_{\theta}^T \Sigma \nabla_{\theta} h_{\theta})\end{aligned}$$

And finally:

$$h_{\hat{\theta}} \rightarrow \mathcal{N}(h_{\theta^*}, \frac{1}{n} \nabla_{\theta} h_{\theta}^T \Sigma \nabla_{\theta} h_{\theta})$$

By estimating $\frac{1}{n}\Sigma$ from `curve_fit`, we can compute the confidence interval of the prediction with the quantiles of the normal distribution. The gradient of h_{θ} is approximated numerically: $\nabla_{\theta} h_{\theta}[i] \simeq \frac{h_{\theta+d\theta_i} - h_{\theta}}{dt}$, with $dt = 0.0001$.

$$d\theta_i = \begin{pmatrix} \theta_0 \\ \theta_1 \\ \vdots \\ \theta_{i-1} \\ \theta_i + dt \\ \theta_{i+1} \\ \vdots \\ \theta_n \end{pmatrix}$$

6 Results and discussion

Metrics

Two metrics were used to assess the performances of the models. The first metric is the Weighted Interval Score (WIS), which is a metric commonly used in forecast evaluation (see [2] or [12]).

Let α be in $]0, 1[$. Let \hat{y} be the prediction of the model and y the real value. Let $[l, u]$ be the $(1 - \alpha)$ confidence interval of the prediction. We define the Interval Score (IS) as:

$$IS_\alpha([l, u], \hat{y}, y) = \frac{2}{\alpha} \times (\mathbb{1}_{\{y < l\}}(l - y) + \mathbb{1}_{\{y > u\}}(y - u) + (u - l)).$$

This metric is made of three terms: a term of overprediction that punishes a model predicting a confidence interval which is above the real value, a term of underprediction that punishes a model whose confidence interval is under the real value, and a term of range, that punishes too wide confidence intervals.

Let $(\alpha_k)_{k \in \{1, \dots, K\}} \in]0, 1[^K$ The WIS is defined as follow.

$WIS([l, u], \hat{y}, y) = \sum_{k=0}^K w_k IS_{\alpha_k}([l, u], \hat{y}, y)$, with $(w_k)_{k \in \{1, \dots, K\}} \in \mathbb{R}_+^K$ weights chosen by the user.

According to previous literature ([2]), I decided to set $(\alpha_k)_{k \in \{1, \dots, K\}} = [0.02, 0.05, 0.1, 0.2, 0.3, 0.4, 0.5, 0.6, 0.7, 0.8, 0.9]$ and $\forall k \in \{1, \dots, K\}, w_k = \frac{\alpha_k}{2}$. One can notice that the WIS does not take into account the point prediction, but focuses on confidence interval accuracy.

The second metric chosen is the Root Mean Square Error ($RMSE$). With the same notations as above, we define the $RMSE$ as follow:

$$RMSE([l, u], \hat{y}, y) = \sqrt{(y - \hat{y})^2}$$

This metric focuses on the point prediction, and does not take into account the confidence intervals.

The models were tested on all the 324 pandemics, on 14 data points different (at days 20, 40, 60, ..., 280). For each individual point, the models were trained on the previous days of the pandemic. A 7 and 14 days ahead prediction was asked, and $[0.02, 0.05, 0.1, 0.2, 0.3, 0.4, 0.5, 0.6, 0.7, 0.8, 0.9]$

confidence-intervals were computed. The WIS and the RMSE of these predictions were then computed. For the analysis of the results, I decided to remove the points for which the number of hospitalized was below 100, as both point classification and model predictions were irrelevant at this period of the pandemic. Moreover, it is senseless to assess the performances of the models during the period in which there is no pandemic, as the interesting models are the ones that can predict the number of hospitalized during the waves. Not removing those points would lead to biased results, as they represent 44% of the dataset, and we would have concluded that the best model is the one that performs well when there is no pandemic.

6.1 Point classification

In order to compare the performance of the models at different point of the pandemic, I have classified the points in six categories: *stable*, *increase*, *big increase*, *decrease*, *big decrease*. The R_{eff} number was used for the point classification. This number is easily available from the Covasim simulation. R_{eff} represents the expected number of people that an infected person will infect. For a pandemic $X_{i,i \in [1, \dots, n]}$ of reproduction number $R_{i,i \in [1, \dots, n]}$, and a day $d \in [1, \dots, n]$, the classification is made according the following rule:

- if $X[d] < 100$:
classification = "no pandemic"
- Elif $R[d] < 0.5$:
classification = "big decrease"
- Elif $R[d] < 0.8$:
classification = "decrease"
- Elif $R[d] < 1.2$:
classification = "stable"
- Elif $R[d] < 3$:
classification = "increase"
- Else:
classification = "big increase"

The values of the thresholds were chosen by hand. As the model are tested on the days [20, 40, 60, ..., 280], we labelled all of these points with the function described above. It resulted that among all those 4536 points, 698 were classified as 'big decrease', 579 as 'decrease', 388 as 'stable', 752 as 'increase', 132 as 'big increase', and 1987 as 'no pandemic'.

6.2 Evaluation of the models

The models described above were tested on 14 points of each of the 324 pandemics generated, when the pandemic was significant (i.e when more than 0.01% of the population was hospitalized, in our case when the value of the number of hospitalized was above 100). For each point, two

predictions were made: a 7-days ahead and a 14-days ahead. Each prediction was evaluated thanks to WIS and RMSE (see 6), and then ranked according to the performances of other models. The points of evaluation were also classified in one of the following categories: 'big increase', 'increase', 'stable', 'decrease' and 'big decrease', based on the value of the reproductive number at this time of the pandemic (see:6.1 for more details). It is then possible to get global information on the rankings of the models. For instance, if the loss and the reach of prediction is fixed, we can look at the distribution of rankings of all the models for a type of point (to see the best model for a type of point), as in Fig.5. This distribution of rankings of the model can

Distribution of the ranks of each model for big increase points for RMSE and 7 days ahead prediction.

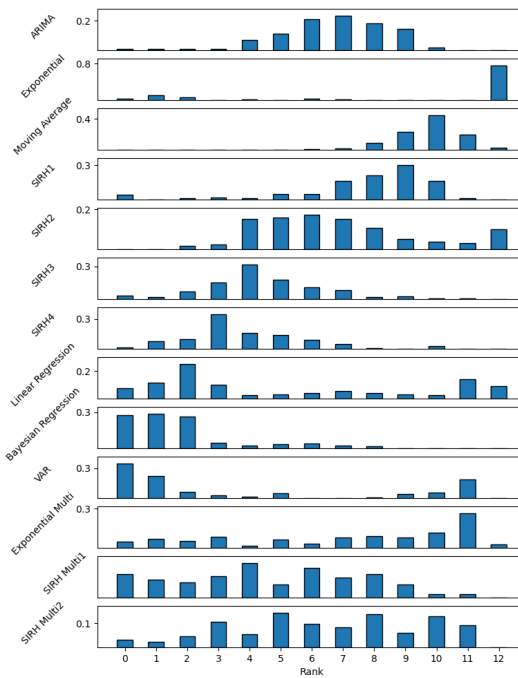


Figure 5: Distribution of rankings of the models for big increase points for 7-days ahead predictions and RMSE loss

be summed up in one single value: the expected value of the rank of a model (see Fig.6), which enables to get the idea of the best model for this type of point, this loss, and this prediction range on a more compact figure.

This new number loses information (for instance on bimodal rankings distribution) but enables to highlight the expected performance of a model. For each loss and range of prediction, the expected rank of the models for each type of point can be visualized on the same figure, which enables to have a global look of the performances of the models.(Fig.7)

The other heatmaps corresponding to RMSE for 14 days ahead prediction and WIS for 7 and 14 days ahead predictions can be found in the appendix (7). Some general interpretations can be made on these results. I noticed that regressors performances drop from 7-days ahead to 14-days ahead. The family of the SIRH model does slightly better for long terms predictions than for short term ones. The ARIMA performance drops from 7-days ahead to 14-days ahead predictions. The exponential models are very bad and almost always the last ones.

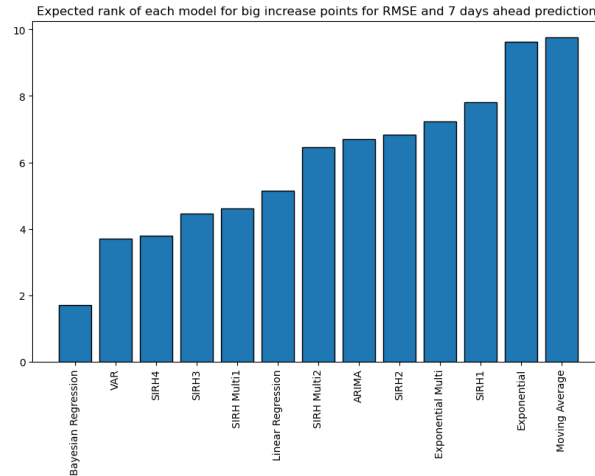


Figure 6: Expected rank of the models for big increase points for 7-days ahead predictions and RMSE loss

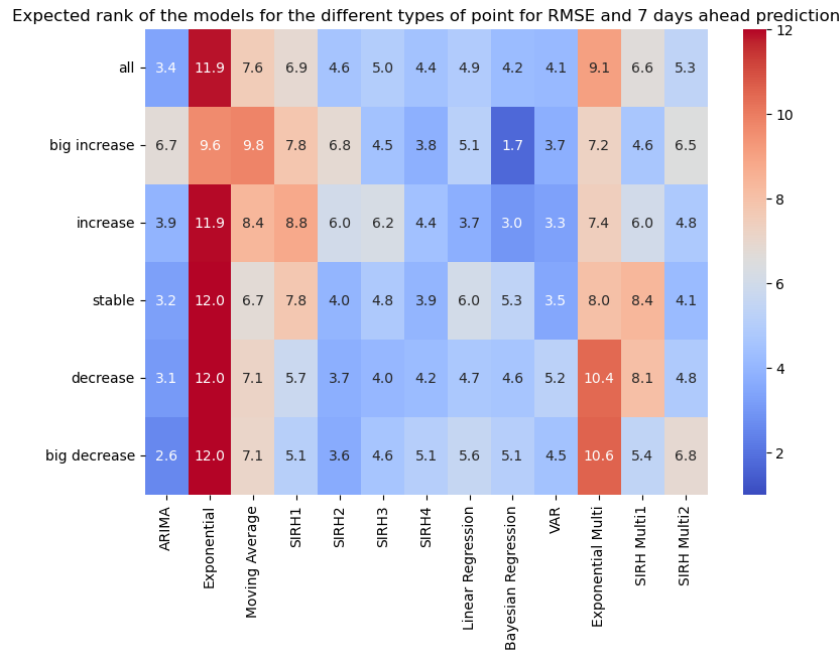


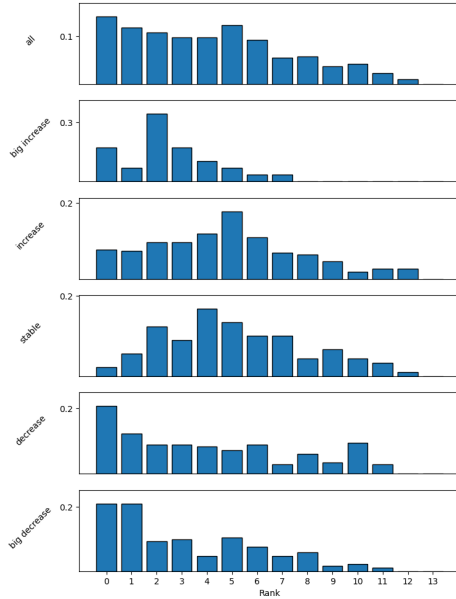
Figure 7: Expected rank of the models for each type of point for 7-days ahead predictions and RMSE loss. For instance, the Bayesian Regression has an average ranking of 1.7 on all the 'big increase' points of the 324 pandemics generated

6.3 The Ensemble model

The performance of the ensemble models have to be separated from the performances of the other models. Indeed, as the ensemble models were trained on a part of the pandemics, they can't be evaluated on the whole set of outbreaks. The performances discussed in this part refer to the same evaluation as above, but only for the RMSE loss and on a test set that represents 20% of the pandemics. The performances of these two models are shown in the two figure below (Fig.8a and Fig.8b)

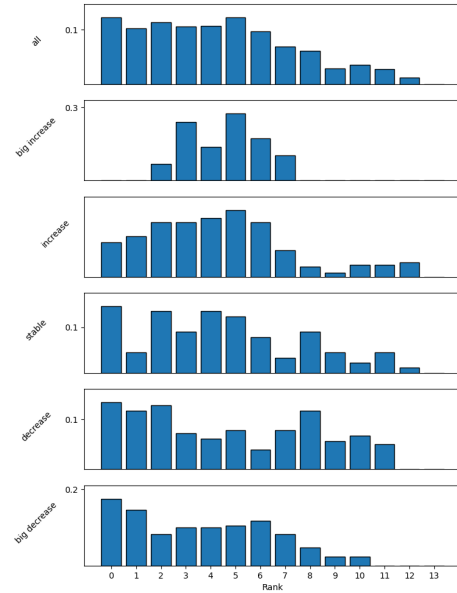
The distribution of the ranks of the ensemble model is almost always on the left side of the x-axis. It is a very consistent model, and almost always in the top models. The heatmaps of

Distribution of the ranks of the Ensemble model for different type of points for 7 days ahead prediction.



(a) Expected rank of the ensemble model for each type of point for 7-days ahead predictions and RMSE loss

Distribution of the ranks of the Ensemble model for different type of points for 14 days ahead prediction.



(b) Expected rank of the ensemble model for each type of point for 14-days ahead predictions and RMSE loss

Figure 8: Comparison of expected ranks for 7-days and 14-days ahead predictions

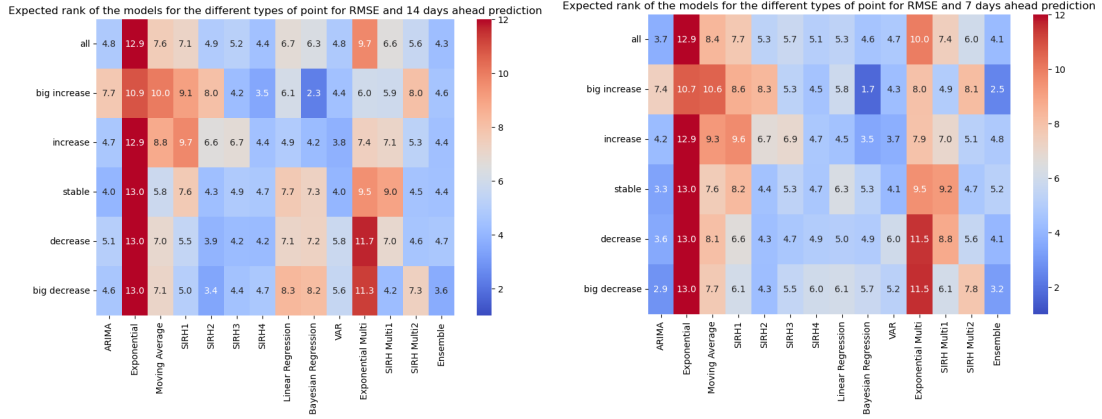
expected ranks on all type of points enables to see how consistent is the ensemble model (Fig.9b and Fig.9a) compared to the other models.

From these figures, one can notice that the ensemble model is rarely the best, but never the last model. Indeed, for a loss, a type of point and a prediction range, one can look at the best models in terms of expected rank. For instance, on the Fig.6, one can see that the top 3 models are Bayesian Regression, VAR and SIRH4. On the train set, the Ensemble model is the only model that appears in all top-6 models for all types of points, all losses and all prediction ranges. Its consistency allows for accurate predictions and helps avoiding outlier predicted values that sometimes appear on the other good models (such as VAR and ARIMA).

6.4 Summary of Key Findings

This method enabled us to assess the consistency of the different models that were implemented. Indeed, comparing the models on a set of diverse pandemics enlightened the most consistent with the different pandemics. Moreover, the classification of the models with the type of points leads to the determination of the phase of the pandemic in which each model is the best, and on the other hand to assess which model is the best for a given R_{eff} . This result is promising, as the reproduction number is a quantity often estimated by the stakeholders during a pandemic. The interpretation based on the heatmaps Fig.10, Fig.7 and Fig.12 and Fig.11 show the following results:

- Arima and VAR are very effective models in terms of expected ranking. They are the two



(a) Expected rank of all the models for each type of point for 14-days ahead predictions (b) Expected rank of all the models for each type of point for 7-days ahead predictions

Figure 9: Expected rank of all the models for each type of point and RMSE loss on the test set for 7-days and 14-days ahead predictions

best models for 7-days ahead predictions and in the top 4 models for the 14-days ahead predictions.

- Adding information with the mobility and the number of infected is not beneficial for the models. We observe almost always a poorer performance of the models of the second type compared to their equivalent model of the first type (VAR / Arima and SIRH Multi / SIRH). Only the exponential multi outperforms the mere exponential model, but as they both perform pretty bad, this result is not interesting.
- The autoregressive models (Bayesian and Linear Regression, ARIMA and VAR) perform best for short term predictions rather than long term ones. On the other hand, the SIRH models, which have a physical meaning and try to fit the data to an understandable model perform better for long term predictions. This is also observed in the coefficients of the ensemble model (see Fig. 4). Indeed, the ensemble model puts more weight on the VAR and Arima models for short term predictions and more on the SIRH models for long terms predictions.
- The difference of ranking between the models is more pronounced when we rank them with RMSE rather than WIS. This might be due to the fact that the confidence intervals are not well calibrated and that the real value always land outside it.
- The Moving Average model is not the worst model and is often ranked between 6 and 8. This might be due to the fact that as the curve of the number of hospitalized is continuous, the mean never diverge too much from the real value, while other models might misinterpret the trend of the curve and land far away from the real value.
- The Exponential models are almost always the last models, except for big increase points that are almost always at the very beginning of the pandemic. the fact that the beginning of a pandemic looks like an exponential curve is also shown with the SIRH model, when the number of infected is very small.

- The Ensemble model performs quite well. I noticed that it is very rarely the best model for a type of point, while other models almost always have some points on which they make the best prediction. On the other hand, it is never the last, and has a very consistent ranking: it is the only model that appears in all top-6 models for all types of points, all losses and all prediction ranges.

6.5 Test on real data

I also tested the models on real data from the Covid-19 pandemic in Sweden and in France. The data of the number of hospitalized individuals was taken from the website Our World in data, the data of the number of infected was taken from the website Worldometers, and the mobility used was the mobility from the Google reports, see [11]. As the mobility used in the previous part concerned public transportation mobility, I decided to focus on the relative mobility in the public transports (*transit_stations_percent_change_from_baseline* in the .csv file provided by Google). The models were tested each 20 days from the 2nd of March to the 7th of December 2020. For each of these points, the models were trained on the data from the beginning of the pandemic to the day before the prediction, and outputed a 7-days ahead and a 14-days ahead prediction. As I wanted to compare the models with the ensemble model, I decided to assess their performances with the RMSE and not the WIS. For each point prediction, the models were ranked according to the RMSE between the prediction and the real value. The rankings are shown on Fig.14. The predictions of the models are plotted with the real data on Fig.15, in the appendix. I noticed similar results to what I observed on the synthetized set for Arima, VAR, Bayesian and Linear regressors: they perform well, but have better results for short term predictions rather than long ones. The performance of the ensemble model is disappointing during the period between the 20th of July and the 8th of October for the Swedish data, but not for the French one, which is surprising, as the curve are both shaped with two waves. Moreover, the Ensemble model puts lots of weight on the VAR model (see fig 4), which might be very sensitive to the errors in the data, as it takes into account the number of infected and the mobility. The difference between this two countries might therefore be due to the quality of the estimation of the number of infected. However, during this "flat" period, even if the ensemble model is not well-ranked, it lands not far from the real value, the other models being better because they are a little closer than him (only for 7 days ahead predictions). On French data, the ensemble model performs well, and is very consistent. The difference of performance between the two countries might also be the consequence of the difference of range of the pandemics due to the difference of population between the two countries.

6.6 Comparison with Previous Research

The very good performance of both VAR and ARIMA models is consistent with previous research. [10] and [18] both assess the performance of the ARIMA model in terms of regional or national prediction accuracy. The interpretation of the coefficients of the ARIMA model enables to have information on the inherent parameters of the pandemic, or to discover links between the different regions of a country. The consistency of the ensemble model has been shown in many previous studies (see [2], [21] and [16]), who also observe that their ensemble model outperformed

any individual model. They also observe the fact that the ensemble model is very consistent: rarely the best, but never the last, allowing to produce robust forecasts. In [15], the authors compared several model to understand they key features that enabled a model to make long term predictions. These features are: " (1) *capturing the physics of transmission (instead of using black-box models)*; (2) *projecting human behavioral reactions to an evolving pandemic*; and (3) *resetting state variables to account for randomness not captured in the model before starting projection*." These findings are consistent with the results that I have observed. Indeed, I have showed that the SEIR model (capturing the physics of transmission and resetting state) performances increase from 7-days ahead to 14-days ahead predictions, while black-box models (such as Arima or VAR), are less effective for long terms prediction. This has to be qualified, as the "long term predictions" of this report refer to a 14-days ahead prediction, while the study [15] get interested to predictions up to 14-weeks reach.

The methodology of point classification has not be found in any other paper of the literature. Some studies assess the performance of the models during different times of a pandemic (see [7]), but this systematic point classification based on the reproduction number was not found.

6.7 Practical Implications

This study might be useful when facing a new pandemic. As the value of the R_{eff} is often estimated by the researchers during a pandemic, it could be used to decide which type of model to use during the current pandemic.

6.8 Limitations

During my researchs, I didn't take into account the impact of uncertainty of the data on the models. Indeed, the Covasim library provided a daily data of high quality and without any noise, but real-life data is often full of mistakes, of missing values or of time-lag in the reports ([6]). It would be interesting to measure the robustness of the models with respect to these imperfections to assess if the models can still make good predictions, and to focus on the robustness of the ensemble model. Moreover, the models of the second type used the number of infected to predict the number of hospitalized. This quantity is not directy accessible and is often estimated with tests, which could lead to huge variations in the predicted values. Finally, the models were only tested on outbreaks generated with Covasim, which might introduce bias in the results, despite the effort to create a diverse set of pandemics.

Conclusion

During my internship, I have tried to reproduce previous results on the consistency of autoregressive and ensemble models, but also to assess the robustness of some models with the evaluation on a huge set of diverse pandemics, which has never been before. The methodology for point classification is also a new way to compare model performnce, that might be useful during real outbreaks, as the reproduction number a popular quantity, which is often estimated. The results of the autoregressive and ensemble models are promising, as many aspects of previous research have been highlighted once again. Future research on the consticency of models with error in

the data might complete this one, by assessing that the observed robustness of the model is not only due to the quality of the data.

References

- [1] T Bodineau. “Modélisation de phénomènes aléatoires: introduction aux chaînes de Markov et aux martingales”. In: *Ecole Polytechnique* (2015).
- [2] Estee Y Cramer et al. “Evaluation of individual and ensemble probabilistic forecasts of COVID-19 mortality in the United States”. In: *Proceedings of the National Academy of Sciences* 119.15 (2022), e2113561119.
- [3] Persi Diaconis. “The markov chain monte carlo revolution”. In: *Bulletin of the American Mathematical Society* 46.2 (2009), pp. 179–205.
- [4] Jasmine M Gardner et al. “Intervention strategies against COVID-19 and their estimated impact on Swedish healthcare capacity”. In: *MedRxiv* (2020), pp. 2020–04.
- [5] Philip Gerlee et al. “Predicting regional COVID-19 hospital admissions in Sweden using mobility data”. In: *Scientific reports* 11.1 (2021), p. 24171.
- [6] Sharon K Greene et al. “Nowcasting for Real-Time COVID-19 Tracking in New York City: An Evaluation Using Reportable Disease Data From Early in the Pandemic”. In: *JMIR Public Health Surveill* 7.1 (Jan. 2021), e25538.
- [7] Emily Howerton et al. “Evaluation of the US COVID-19 Scenario Modeling Hub for informing pandemic response under uncertainty”. In: *Nature communications* 14.1 (2023), p. 7260.
- [8] Henrik Hult and Martina Favero. “Estimates of the proportion of SARS-CoV-2 infected individuals in Sweden”. In: *arXiv preprint arXiv:2005.13519* (2020).
- [9] Cliff C Kerr et al. “Covasim: an agent-based model of COVID-19 dynamics and interventions”. In: *PLOS Computational Biology* 17.7 (2021), e1009149.
- [10] Tadeusz Kufel. “ARIMA-based forecasting of the dynamics of confirmed Covid-19 cases for selected European countries”. In: *Equilibrium. Quarterly Journal of Economics and Economic Policy* 15.2 (2020), pp. 181–204.
- [11] Google LLC. *Google COVID-19 Community Mobility Reports*. <https://www.google.com/covid19/mobility/>. Accessed: July 10, 2024.
- [12] Juliette Paireau et al. “An ensemble model based on early predictors to forecast COVID-19 health care demand in France”. In: *Proceedings of the National Academy of Sciences* 119.18 (2022), e2103302119.
- [13] Victor M Panaretos and Yoav Zemel. “Statistical aspects of Wasserstein distances”. In: *Annual review of statistics and its application* 6.1 (2019), pp. 405–431.
- [14] James Powell. “Asymptotics for least squares”. In: ().
- [15] Hazhir Rahmandad, Ran Xu, and Navid Ghaffarzadegan. “Enhancing long-term forecasting: Learning from COVID-19 models”. In: *PLoS computational biology* 18.5 (2022), e1010100.
- [16] Nicholas G Reich et al. “Accuracy of real-time multi-model ensemble forecasts for seasonal influenza in the US”. In: *PLoS computational biology* 15.11 (2019), e1007486.

- [17] Andreas Ruckstuhl. “Introduction to nonlinear regression”. In: *IDP Institut für Datenanalyse und Prozessdesign, Zürcher Hochschule für Angewandte Wissenschaften* (2010), p. 365.
- [18] Aaron C Shang, Kristen E Galow, and Gary G Galow. “Regional forecasting of COVID-19 caseload by non-parametric regression: a VAR epidemiological model”. In: *AIMS public health* 8.1 (2021), p. 124.
- [19] Henrik Sjödin et al. “COVID-19 healthcare demand and mortality in Sweden in response to non-pharmaceutical mitigation and suppression scenarios”. In: *International journal of epidemiology* 49.5 (2020), pp. 1443–1453.
- [20] Charles SUQUET. “Lois des grands nombres”. In: *Université des Sciences et Technologies de Lille* (2004).
- [21] Cécile Viboud et al. “The RAPIDD ebola forecasting challenge: Synthesis and lessons learnt”. In: *Epidemics* 22 (2018). The RAPIDD Ebola Forecasting Challenge, pp. 13–21. ISSN: 1755-4365.

7 Appendix

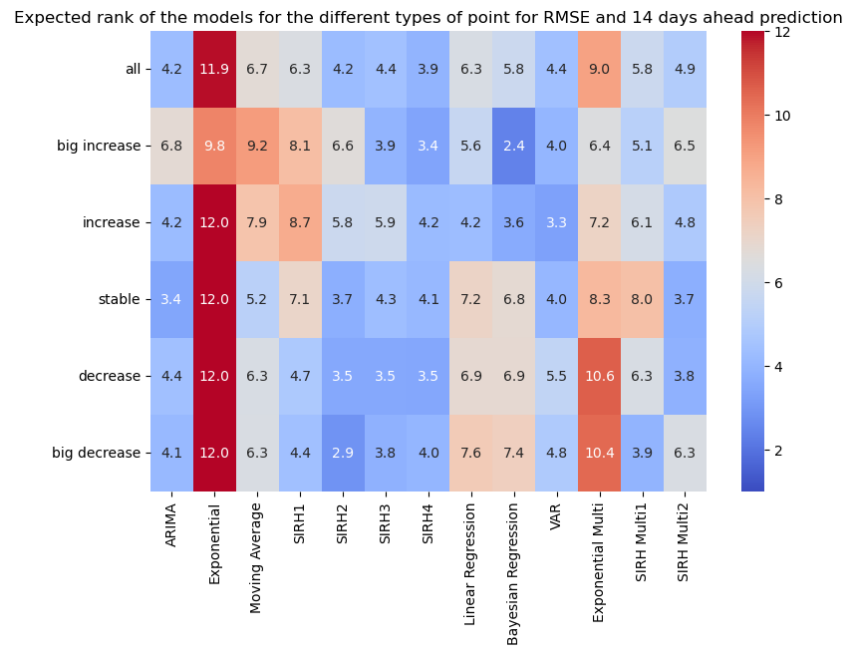


Figure 10: Expected rank of the models for each type of point for 14-days ahead predictions and RMSE loss

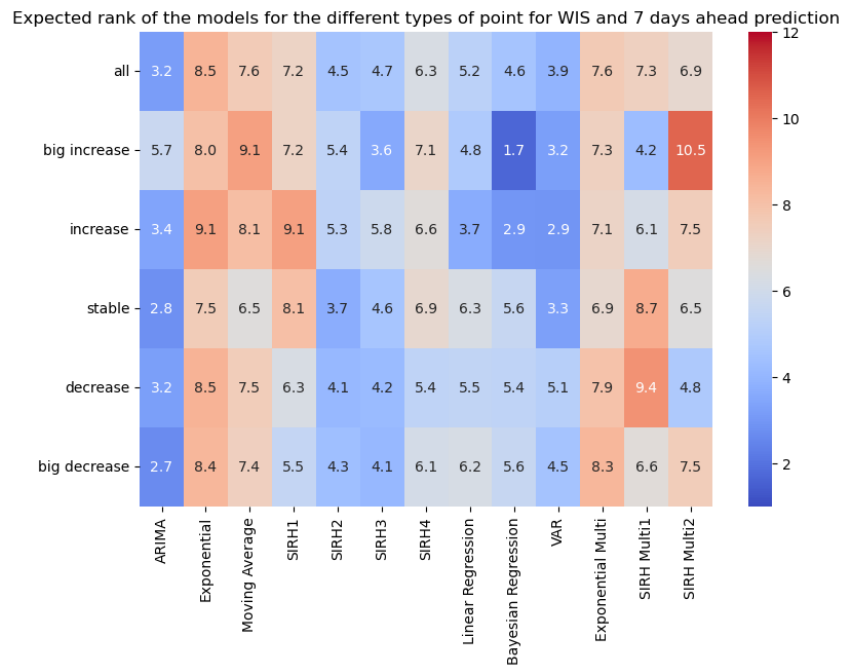


Figure 11: Expected rank of the models for each type of point for 7-days ahead predictions and WIS loss

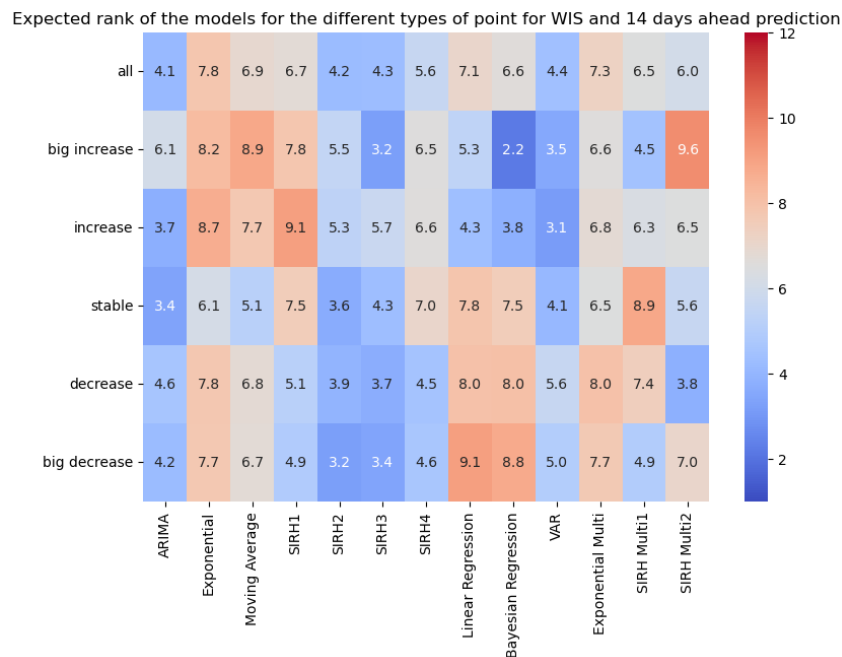


Figure 12: Expected rank of the models for each type of point for 14-days ahead predictions and WIS loss

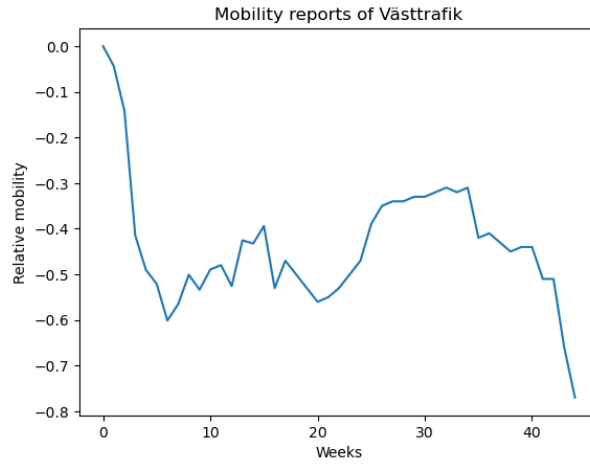
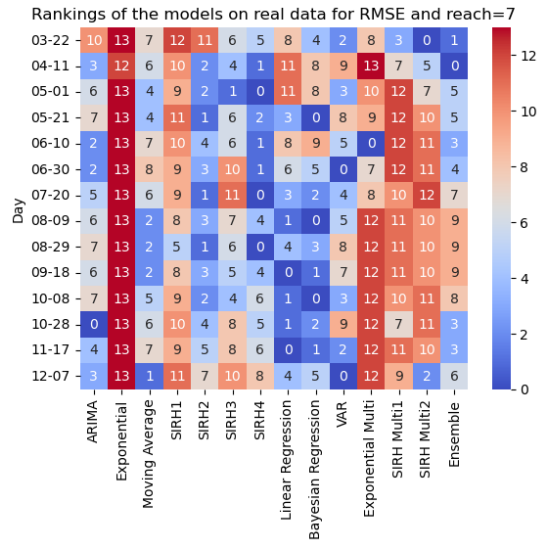
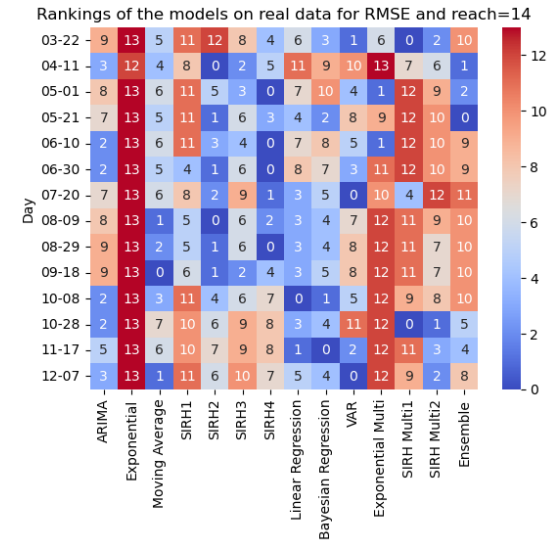


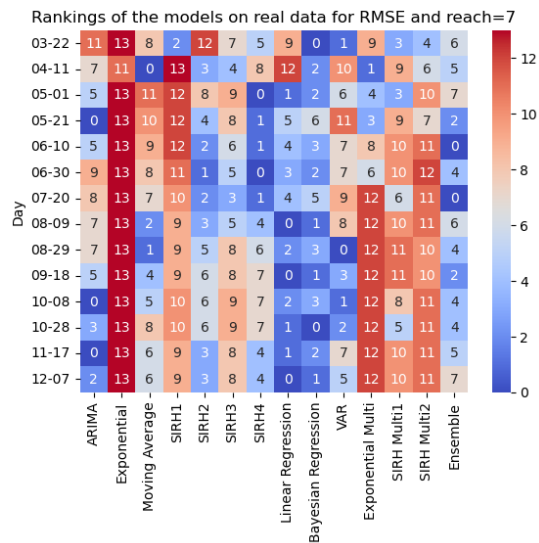
Figure 13: Mobility reports.



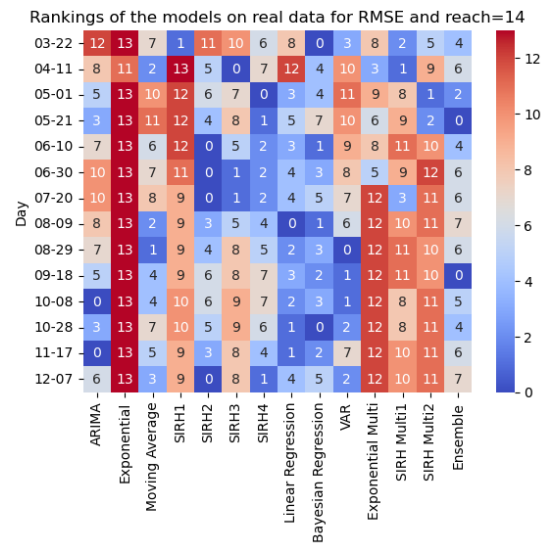
(a) Rankings for 7-days ahead predictions for Sweden



(b) Rankings for 14-days ahead predictions for Sweden

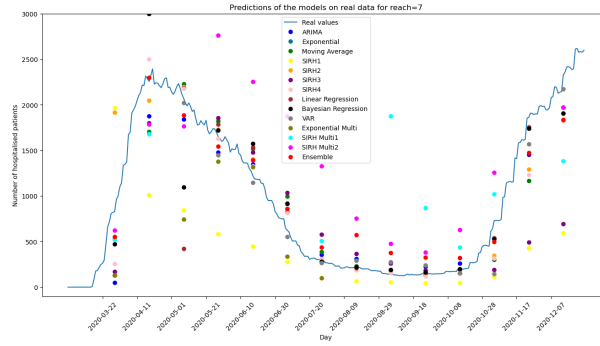


(c) 7-days ahead predictions for France

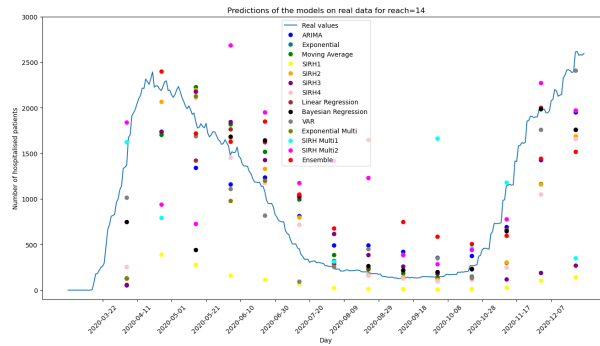


(d) 7-days ahead predictions for France

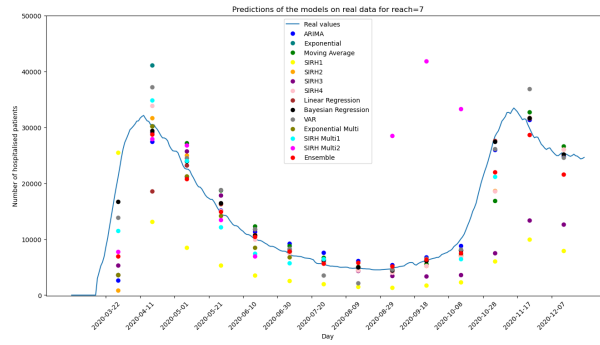
Figure 14: Rankings of the models during the Covid-19 pandemic in Sweden



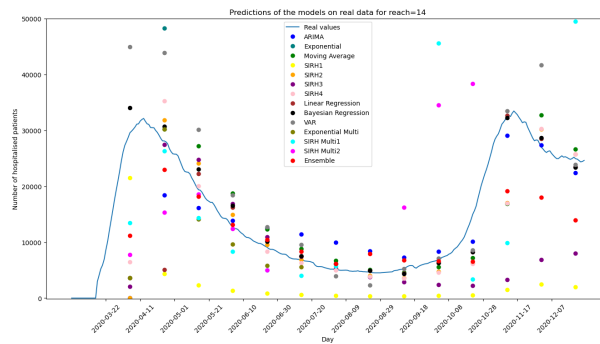
(a) 7-days ahead predictions for Swedish data



(b) 14-days ahead predictions for Swedish data



(c) 7-days ahead predictions for French data



(d) 14-days ahead predictions for French data

Figure 15: Predictions of the models during the Covid-19 pandemic in Sweden and France.